

1994

# Comparison of Mixing Devices for Flow Injection Determinations Based on Doublet Peak Formation

Julian Tyson

*University of Massachusetts Amherst*

RT Echols

*University of Massachusetts Amherst*

Follow this and additional works at: [https://scholarworks.umass.edu/chem\\_faculty\\_pubs](https://scholarworks.umass.edu/chem_faculty_pubs)

 Part of the [Chemistry Commons](#)

---

## Recommended Citation

Tyson, Julian and Echols, RT, "Comparison of Mixing Devices for Flow Injection Determinations Based on Doublet Peak Formation" (1994). *Analytica Chimica Acta*. 1311.

Retrieved from [https://scholarworks.umass.edu/chem\\_faculty\\_pubs/1311](https://scholarworks.umass.edu/chem_faculty_pubs/1311)

This Article is brought to you for free and open access by the Chemistry at ScholarWorks@UMass Amherst. It has been accepted for inclusion in Chemistry Department Faculty Publication Series by an authorized administrator of ScholarWorks@UMass Amherst. For more information, please contact [scholarworks@library.umass.edu](mailto:scholarworks@library.umass.edu).

# Comparison of mixing devices for flow-injection determinations based on doublet peak formation

Roger T. Echols and Julian F. Tyson

*Chemistry Department, University of Massachusetts, Amherst, MA 01003 (USA)*

(Received 5th August 1993; revised manuscript received 4th October 1993)

## Abstract

The well-stirred tank model accurately describes the separation ( $\Delta t$ ) between flow-injection doublet peaks and has been found to be applicable to a variety of mixing devices that do not contain moving parts such as a magnetic follower. The reaction between lanthanum(III) and methyl thymol blue was used as a model reaction for a comparison study of mixing devices. Column and open-tubular reactors were included in the study. Mixing devices were compared on the basis of the straight line fit of  $\Delta t$  versus the natural logarithm of the concentration of injected La(III). The linearity of the  $\Delta t - \ln[\text{La(III)}]$  plots was equivalent for several reactors. A mixing device composed of a column of alternating helices was selected as the best alternative mixer to the well-stirred tank when the magnitude of the slope of the plot and practicality were considered. Experiments showed that the well-stirred tank model qualitatively describes the behavior of these alternating helical reactors (AHR) in experiments designed to produce doublet peaks. The AHR was used as the mixing device in flow-injection determinations, based on doublet peaks, of zinc, hydroxide ion and of water hardness. A paired *t*-test showed that over the 16 determinations performed there was no significant bias at the 95% confidence level. Factors affecting the relative standard deviation of the concentrations measured are discussed.

*Keywords:* Flow injection; Double peak formation; Mixing devices

The interest over the past decade in time-based and kinetic flow-injection (FI) methods has been a natural extension of FI because of the inherent kinetic nature of such methods [1,2]. Time-based flow-injection methods of analysis have received attention as alternatives to traditional FI methods, which have relied on peak height as the quantitative analytical parameter. The increased linear range of determination of several orders of magnitude and speed of analysis have been cited as advantages of these methods [3,4].

For time-based methods an interval of time between data points on the concentration–time profile is used as the quantitative analytical pa-

rameter. Common examples of time-based FI methods are those based on a change in concentration over time under conditions of stopped-flow [1,2]. Reactions monitored in stopped-flow methods must be slow relative to the time scale of the flow system. For other time-based methods such as peak-width methods, chemical kinetics of a reaction are not considered. Reactions are sufficiently fast such that dispersion is the only phenomenon contributing to the concentration gradient of the injected sample. There has been some debate over the nomenclature used to identify these methods. In this paper, peak-width methods involving the measurement of doublet peaks will be considered a subset of time-based methods. Other time-based methods have been based upon measurement of a time interval between

*Correspondence to:* J.F. Tyson, Chemistry Department, University of Massachusetts, Amherst, MA 01003 (USA).

points on any part of the peak profile [5]. Determinations based on the time between doublet peaks will also be referred to as "flow-injection titrations" because the term has been used previously [1–6] and is descriptive as to the kinds of chemistry [7] that can be exploited by FI time-based methods.

The use of doublet peaks as the analytical parameter of interest is in keeping with the general philosophy of FI, that of providing an easily identifiable quantitative parameter. The most common analytical parameter is peak height, for which operating conditions of the flow system are adjusted so that doublet peaks are avoided [1]. Flow-injection doublet peaks are obtained when conditions of the FI system are adjusted so that the injected sample material is in excess over the carrier stream in the center of the injected slug. Under conditions of a fast reaction and no diffusion, the product profile matches the sample profile, except in the center region. Two peaks arise from the pair of increasing and decreasing product concentration gradients. For a well-stirred tank, the gradient is exponential such that there is a semilogarithmic relationship between time and the concentration of injected analyte.

The mathematical relationship between time between doublet peaks and concentration is based on a model of plug flow of injected sample through a well-stirred mixing chamber [5]. The time interval ( $\Delta t$ ) between doublet peaks is given by

$$\Delta t = (V/Q) \ln C_s + (V/Q) \times \ln[\{\exp(V_i/V) - 1\}/C_r] \quad (1)$$

in which  $V$  is the volume of the mixing chamber,  $Q$  is the flow rate,  $C_s$  is the concentration of the injected sample,  $C_r$  is the concentration of the reagent solution, and  $V_i$  is the volume of the injected sample. A plot of  $\Delta t$  versus  $\ln C_s$  is linear with a slope of  $V/Q$ .

Two other theoretical treatments have led to the semilogarithmic relationship between time and the concentration of injected sample. Ruzicka et al. [3] used a tanks-in-series model and the concept of dispersion to derive equations relating time and analyte concentration. Points on the rise

and fall curves of FI peaks were used in measuring the interval of time, which was related through a calibration plot to the logarithm of concentration. An acid–base system and a calcium–EDTA system illustrated the new method, which was termed FI titration. A complexometric titration and oxidation–reduction titration were demonstrated in a subsequent paper in which a tubular reactor was employed as the mixing device [6].

Pardue and co-workers [8–12] have derived equations that relate time intervals to analyte concentrations using a variable-time kinetic model; the last paper is a thorough overview [12]. The authors derived equations for several experimental situations and discussed using peak widths obtained from a variety of reference points on the FI concentration–time profile. Mathematical relationships between peak width and  $\ln C_s$  are, in general, nonlinear. However, an approximately linear relationship is obtained for situations in which the reference point concentrations (between which the peak width is measured) are much less than injected analyte concentrations. Recent work by Jordan and Pardue [13] has shown that it is possible to obtain excellent agreement between experiment and theory for FI systems in which the dispersion behavior is dominated by the concentration gradients produced by a single well-stirred mixing chamber. They evaluated a variety of methods in which data from such FI experiments can be manipulated to give quantitative analytical parameters for the situation in which the product profile is monitored under conditions in which the reagent is always in excess [14]. An acid–base reaction, the triiodide–thiosulfate reaction and the iodate–iodide reaction were the chemical systems used in these studies [8–14].

Previous work has shown that Eqn. 1 is valid for experimental conditions that result in the formation of doublet peaks [4,5]. A well-stirred mixing chamber was used in the experiments correlating experimental data with parameters in Eqn. 1, but a gradient tube was used in the experiments designed to illustrate the linear dynamic range of FI titrations [4]. It has also been shown possible to determine stability constants from doublet peak data [15]. Recent work in our

laboratory has focused on the development of inexpensive detectors for undergraduate teaching experiments based on the measurement of time between doublet peaks [16–18]. LEDs (light-emitting diodes) and laser diodes were employed as light sources in this work; simple electronic circuitry was used to measure  $\Delta t$  values.

In this paper the study of practical mixing devices for FI methods based on the formation of doublet peaks is continued. Results from an investigation of a variety of FI reactors, which do not contain moving parts (such as the magnetic follower of a well-stirred tank) are presented. The linear fit of  $\Delta t - \ln C_s$  plots and practical considerations of the application of the mixing devices are criteria for choosing one static mixer as the best mixer for further study. The applicability of Eqn. 1 to FI doublets produced under non-well-stirred tank conditions is discussed and the application of static mixers for simple determinations by FI titrations is illustrated with simple chemical systems.

## EXPERIMENTAL

### Apparatus

**Flow-Injection System.** A single-line flow-injection manifold was used in all experiments (Fig. 1). Components included a variable speed peristaltic pump (Ismatec sa), a six-port injection valve (Rheodyne, an 8- $\mu$ l flow cell (Hellma), and a UV-visible detector (Novaspec). An integrator (Hewlett-Packard Model HP 3394A) was used for data collection. All flow tubing was 0.8 or 0.9 mm

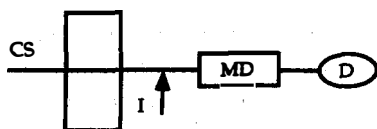


Fig. 1. Basic flow-injection manifold used in all experiments. CS, carrier stream; I, injection valve; MD, mixing device; D, detector. For the model reaction, La(III) is introduced at I into a carrier stream of methyl thymol blue. The reaction is monitored at 608 nm.

i.d. PTFE tubing. Slug injection was employed in all experiments; injected volume and flow rates were varied and are noted below.

**Mixing devices.** Mixing devices (static mixers) were obtained from a number of sources. With the exception of the short tube and the roughened flow tubing, 0.8 mm i.d. flow tubing was used to construct the tubular reactors. A 15 cm  $\times$  2 mm i.d. PTFE tube was employed as the short tube. Roughened tubing was obtained from Life-source Ventures (Atlanta, GA). Mixing chambers were used in previous work [4]. The empty Omni column was obtained from Omnifit. The packed reactor consisted of 250  $\mu$ m glass spheres packed in a 6 cm  $\times$  2 mm i.d. PTFE tube; single-bead string reactors consisted of glass spheres of 500–600  $\mu$ m diameter in 0.8 mm i.d. tubing. Alternating helical reactors (AHR) were constructed from 3/16 in. i.d. plastic helical segments inserted into lengths of 0.6 cm i.d. tubing. Flow through the reactors is disturbed by the helical segments. The helical segments are available from Cole-Parmer as “in-line static mixers.” The “prototype” static mixer, also a reactor that contains segments that disturb the flow pattern, was obtained courtesy of Upchurch.

### Reagents

**Lanthanum–methyl thymol blue reaction.** Buffered lanthanum solutions ( $1.13 \times 10^{-2}$  M to  $1.41 \times 10^{-5}$  M) were prepared from a  $1.8799 \times 10^{-2}$  M lanthanum chloride stock solution, which was standardized against EDTA. Solutions were buffered with an acetic acid–acetate buffer that was prepared by adjusting the pH of a 0.005 M sodium acetate solution to 6.2. Methyl thymol blue (MTB) solutions were also prepared in the acetate buffer at a concentration of around  $3 \times 10^{-5}$  M. Preparation of MTB solutions of exactly known concentrations was difficult due to the purity of the Aldrich reagent grade MTB (95% purity).

**Zinc–methyl thymol blue reaction.** Zinc solutions were prepared by dilution from a standardized zinc sulfate stock solution of  $4.2828 \times 10^{-1}$  M. Solutions were buffered with 0.005 M acetate buffer (pH 6.0). A buffered MTB solution of  $4 \times 10^{-5}$  M (pH 6.0) was used as the reagent.

*Hydrochloric acid–sodium hydroxide reaction.* Sodium hydroxide solutions were prepared from a NaOH stock solution of 1.5512 M, which was standardized versus KHP. The carrier stream for the acid–base titration consisted of  $8.9 \times 10^{-4}$  M HCl and approximately  $3 \times 10^{-5}$  M bromothymol blue (BTB) indicator.

*Magnesium / calcium–EDTA reaction.* Calcium and magnesium solutions were prepared from standardized 0.2893 M and 0.3743 M stock solutions of the nitrate salts. Each solution contained about 0.1% calmagite indicator solution. The  $2.030 \times 10^{-3}$  M EDTA carrier stream was prepared by dissolution of the dried acid. All solutions were buffered with 10% of a pH 10.1 ammonia–ammonium buffer stock solution.

### Procedures

#### *Study of reactors used to produce doublet peaks.*

The colorimetric reaction between lanthanum and MTB was used in the study of mixing devices. Mixing devices were compared on the basis of the straight line fit of the plot of time between doublet peaks ( $\Delta t$ ) versus the natural logarithm of concentration (in units of ppm) of La(III). Three or four replicate injections of each concentration were made for all mixers. In some cases a doublet peak was not produced and the data points were not used in the plot. The variance of the  $\Delta t$  residuals ( $s_{y/x}^2$ ), correlation coefficient squared, intercept, slope and the confidence interval of the slope [19,20] were calculated for each mixing device using Statview (BrainPower). The goals of the study did not require that the volume injected and flow rate need be the same for all mixing devices, although reasonable values of injected volume were used and efforts were made to maintain the flow rate at approximately  $27 \mu\text{l/s}$ .

Reactor volumes were obtained by acid–base titration. The mixing device was filled with a Tris solution of known concentration and eluted into an Erlenmeyer flask; standardized HCl was used as a titrant. Flow rate was determined by measuring the time required to collect 10 ml of eluent in a calibrated flask.

#### *Characterization of alternating helical reactors.*

The behavior of static mixers with respect to that

TABLE 1

Experimental parameters

Carrier	Analyte	Conc. of standards (M)	$V$ ( $\mu\text{l}$ )	$V_i$ ( $\mu\text{l}$ )	$Q$ ( $\mu\text{l/s}$ )
1 MTB	Zinc	$1.03 \times 10^{-5}$ – $3.43 \times 10^{-3}$	1581	1494	26.0
2 HCl	NaOH	$6.21 \times 10^{-4}$ – $3.10 \times 10^{-1}$	384	507	23.8
3 EDTA	Mg/Ca	$5.99 \times 10^{-4}$ – $1.50 \times 10^{-2}$	1581	1211	26.2

expected from theory [4] was investigated using the model reaction and the static mixers. Flow rate was varied from  $18 \mu\text{l/s}$  to  $39 \mu\text{l/s}$  for a 15 segment AHR; mixer volume was varied from  $384 \mu\text{l}$  to  $1860 \mu\text{l}$  for six AHRs.

*Flow-injection titrations using alternating helical reactors.* Three simple chemical systems were used to demonstrate flow-injection determinations based on doublet peaks: the complexometric reaction between zinc and MTB, the acid–base reaction between HCl and NaOH, and the traditional water-hardness titration reaction, magnesium and calcium–EDTA with calmagite indicator. Data were collected for a range of standards; calibration plots were used to determine concentration of synthetic unknowns. Conditions for these determinations are listed in Table 1. The three example reactions were chosen to illustrate different ways doublet peaks can be formed. For the Zn–MTB reaction, the product profile is monitored at 580 nm. For the acid–base reaction, the absorbance–time profile of BTB is monitored at 620 nm. For the third reaction, the absorbance of an indicator, calmagite, is monitored at 675 nm. Calmagite is participating in the ligand exchange reaction:



For the latter two chemical systems, the BTB and calmagite indicators, which are the chemical species being monitored spectrophotometrically, are not the reaction products. For these reactions, it is assumed that the absorbance maxima of the indicators correspond in the time domain to the concentration maxima (“doublet peaks”) of the product (see introductory part).

## RESULTS AND DISCUSSION

### Model reaction

Preliminary work has shown that diffusion effects are possible reasons for experimental error in acid–base doublet peak experiments; thus, a complexometric reaction rather than an acid–base reaction was selected as the model reaction. The reaction between lanthanum(III) and methyl thymol blue was chosen for the comparison study of mixing devices for the following reasons. The product of the reaction absorbs at 608 nm, a wavelength at which the molar absorptivity of the free ligand is low, the reaction is rapid and the reaction is reported to have a 1:1 stoichiometry and a conditional formation constant of  $10^6$  (pH 6.5) [21]; another study has reported a conditional formation constant of  $10^{7.4}$  (pH 5.84) for a 2:2 reaction product [22]. The range of La(III) concentrations employed in the study was established at the low end by a concentration that yielded resolvable doublet peaks and at the high end by the concentration for which a peak maximum could be detected on the second peak of the

doublet. The range of applicable solutions varied between reactors.

### Comparison of mixing devices

Results from the comparison of mixing devices are enumerated in Table 2. The variance of the  $\Delta t$  residuals,  $s_{y/x}^2$ , is the parameter of merit for comparing the behavior of the mixing device to that expected from theory (i.e., a linear plot of  $\Delta t$  versus  $\ln C_s$ ). The square of the correlation coefficient is not as sensitive to differences among mixers and thus was not chosen as the parameter of merit. The scatter of  $\Delta t$  values from replicate injections and the non-linearity of the data is reflected in  $s_{y/x}^2$ . In most cases the standard deviations of replicate injections were low; thus, the data reflects deviation of  $\Delta t$  values from the linear least squares best-line fit. Examination of Table 2 reveals that there is little difference between the linear fit of many of the mixing devices. With the exception of the empty column reactor and the larger volume coiled reactor, all mixing devices fit the theory as well as or better than the well-stirred tanks. It should be noted

TABLE 2

Summary of results for various mixing devices

Mixing device	$s_{y/x}$	$s_{y/x}^2$	$R^2$	Intercept (s)	Slope ( $\pm 95\%$ CI) (s)	$V$ ( $\mu\text{l}$ )	$V_i$ ( $\mu\text{l}$ )	$Q$ ( $\mu\text{l/s}$ )	Slope $\times Q$ $V_{\text{eff}}$ ( $\mu\text{l}$ )
Well-stirred tank I	1.934	3.740	0.997	-25.83	25.67 ( $\pm 0.96$ )	828	783	25.25	648.1
Prototype static mixer I	0.741	0.549	0.996	1.55	5.56 ( $\pm 0.19$ )	267	374	27.17	151.0
Knotted reactor I	0.842	0.709	0.992	5.52	3.97 ( $\pm 0.18$ )	400	374	28.46	113.0
Prototype static mixer II	0.616	0.379	0.998	15.77	6.29 ( $\pm 0.16$ )	267	783	27.75	174.5
Coiled tubing	1.584	2.509	0.979	3.20	5.24 ( $\pm 0.41$ )	428	374	27.73	145.3
Fat tube reactor	1.455	2.117	0.989	-0.38	5.93 ( $\pm 0.30$ )	242	374	27.50	163.0
Uncoiled tubing	1.353	1.831	0.985	1.93	5.42 ( $\pm 0.35$ )	428	374	28.31	153.3
Roughened tubing I	1.340	1.796	0.992	-2.57	7.25 ( $\pm 0.35$ )	556	374	27.36	198.2
Roughened tubing II	1.616	2.611	0.977	2.93	5.33 ( $\pm 0.45$ )	417	374	28.36	151.3
Column reactor (Omni)	2.773	7.690	0.982	-10.49	11.58 ( $\pm 1.08$ )	748	507	27.39	317.1
Well-stirred tank II	2.270	5.153	0.993	6.84	10.82 ( $\pm 0.56$ )	378	802	28.19	305.0
Knotted reactor II	1.206	1.454	0.989	5.60	5.60 ( $\pm 0.30$ )	1270	507	29.01	162.4
None	0.584	0.341	0.992	7.85	2.73 ( $\pm 0.15$ )	n/a	374	28.50	77.7
Tight coiled tubing	2.924	8.550	0.968	23.01	7.84 ( $\pm 0.92$ )	891	802	29.03	227.6
Packed bed reactor	0.885	0.783	0.991	9.01	4.42 ( $\pm 0.28$ )	96	374	20.82	92.0
SBSR-I	0.459	0.211	0.995	7.96	3.28 ( $\pm 0.10$ )	192	374	25.58	84.0
SBSR-II	0.468	0.219	0.997	9.47	4.56 ( $\pm 0.12$ )	384	507	27.28	124.4
AHR 3 segments	0.767	0.588	0.997	2.96	6.28 ( $\pm 0.16$ )	384	507	33.23	208.7
AHR 6 segments	1.052	1.107	0.998	5.53	9.57 ( $\pm 0.22$ )	696	783	31.21	298.8

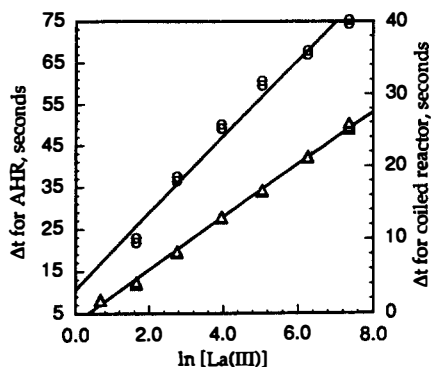


Fig. 2. Calibration plot ( $\Delta t$  vs.  $\ln[\text{La(III)}]$ ) for two static mixers:  $\circ$  = 60 cm  $\times$  0.8 mm i.d. coiled tubing reactor;  $\Delta$  = 3-segment alternating helical reactor. Note curvature in plot of data collected using the coiled tubing as mixing device.

that much of the error in the estimated values for the stirred tank was as a result of the large scatter of replicate  $\Delta t$  values around the mean  $\Delta t$  values. The linear fit of the mean  $\Delta t$  values for the well-stirred tanks was excellent.

The mixing devices with the lowest  $s_{y/x}^2$  values were those reactors that were expected to enhance radial dispersion and reduce axial dispersion [1]: knotted reactors, packed reactor, single-bead string reactors and the alternating helical reactors. Surprisingly,  $s_{y/x}^2$  for no mixer (absence of a mixer) was low, but it was excluded from further consideration because of the low value of the slope. Examination of plots of  $\Delta t$  versus the natural log of La(III) concentration indicated that there was curvature in the plots (Fig. 2) for some reactors. This has been observed in other work [14] and was expected for mixing devices such as the coiled reactor. Application of the Wald-

Wolfowitz runs test [18] confirmed the curvature for these static mixers.

Perhaps the only conclusion to draw from the above discussion is that a variety of reactors, which disrupt the flow and enhance the radial dispersion, behave like well-stirred tanks for the purpose of establishing a linear relationship between the separation doublet peaks and the logarithm of injected concentration. Adherence to Eqn. 1 is limited to the linear relationship of the slope; data is not expected to validate the model to the extent that was presented earlier for a well-stirred experimental system [4]. A comparison of the actual volumes and effective volumes ( $V_{\text{eff}}$ ) (Table 2) illustrates the lack of correlation between experimental and theoretical results.

The  $F$ -test (ratio of variances) was used to test for differences between  $s_{y/x}^2$  of differing reactors. With the exception of the variance of the SBSRs, the variance of the packed reactor, the lowest-volume knotted reactor, prototype static mixer and AHRs were not statistically different. Given the reduced list of possible alternatives to the well-stirred tank, other criteria were imposed: the slope of the  $V/Q$  plot and practicality. The slope of the calibration plot is important in determinations based on the width of doublet peaks and will be discussed below. The prototype static reactor had a low volume, which could not be increased. Thus, only knotted reactors, single-bead string reactors, packed reactors and AHRs were considered. Increasing the volume of the knotted reactors and SBSRs did not increase the slope of the  $\Delta t$  vs.  $\ln C_s$  plots by a significant amount. From a stand-point of practicality, the packed reactor was eliminated from considera-

TABLE 3

Results for alternating helical reactors

No. of segments	Intercept (s)	Slope ( $\pm 95\%$ CI) (s)	$V$ ( $\mu\text{l}$ )	$V_i$ ( $\mu\text{l}$ )	$Q$ ( $\mu\text{l/s}$ )	$V_{\text{eff}}$ ( $\mu\text{l}$ )
3	2.96	6.28 ( $\pm 0.16$ )	384	507	33.23	208.7
6	5.53	9.57 ( $\pm 0.22$ )	696	783	31.21	298.8
9	15.24	12.38 ( $\pm 0.43$ )	966	1211	30.35	375.7
12	10.98	14.54 ( $\pm 0.22$ )	1283	1211	30.07	437.2
15	11.51	18.03 ( $\pm 0.27$ )	1581	1494	30.81	555.5
18	8.89	19.09 ( $\pm 0.19$ )	1860	1494	30.89	589.8

tion because of difficulty in construction and difficulties with back-pressure. Further, construction of SBSRs was time-consuming and tedious, while the volume for AHR reactors is easily adjusted with a longer length of tubing and a greater number of helical segments. Experiments varying the volume showed that the slope of the regression plot did increase with increasing AHR volume. On the basis of this, and with consideration of the practicality, AHRs were chosen as the best alternative mixing device to well-stirred tanks.

#### Characterization of alternating helical reactors

Results from experiments varying the volume and flow rate of the alternating helical reactors are shown in Table 3. Adherence of the AHRs to the well-stirred tank model is indicated in Figs. 3

and 4. The slope of the plot of  $\Delta t$  versus  $\ln C_s$  increases with reactor volume and increases as a function of the inverse flow rate ( $1/Q$ ). It is important not to conclude that AHRs are behaving like well-stirred tanks. Significant differences exist between the volumes of the AHRs and their calculated effective volumes (product of the slope and the flow rate); further, there is little correlation between experimentally and theoretically obtained values for  $V_i$  and  $C_r$ . Figures 3 and 4 reveal that AHRs approximate the behavior of well-stirred tanks, providing sufficient mixing to allow Eqn. 1 to be used for determinations based on peak-width of doublet peaks.

The practical information derived from these results is what is important. The slopes of  $\Delta t$  versus  $\ln C_s$  plots can be changed (typically increased) by changing the number of segments

TABLE 4  
Results for flow-injection titrations

Analyte/unknown No.	$\Delta t$ (s)	Analyte content (M)	Analyte found (M)	Percent difference
<i>Zn</i>				
1	63.78	$6.852 \times 10^{-5}$	$6.947 \times 10^{-5}$	1.4
2	135.97	$1.713 \times 10^{-3}$	$1.632 \times 10^{-3}$	-4.7
3	46.96	$3.427 \times 10^{-5}$	$3.330 \times 10^{-5}$	-2.8
4	121.12	$8.565 \times 10^{-4}$	$8.524 \times 10^{-4}$	-0.5
5	129.18	$1.199 \times 10^{-3}$	$1.213 \times 10^{-3}$	1.2
<i>NaOH</i>				
1	56.22	$3.102 \times 10^{-2}$	$3.223 \times 10^{-2}$	3.9
2	41.84	$9.307 \times 10^{-3}$	$8.979 \times 10^{-3}$	-3.5
3	17.43	$9.928 \times 10^{-4}$	$1.027 \times 10^{-3}$	3.4
4	34.46	$4.964 \times 10^{-3}$	$4.661 \times 10^{-3}$	-6.1
<i>Mg</i>				
1	92.50	$1.123 \times 10^{-2}$	$1.091 \times 10^{-2}$	-2.8
2	62.30	$3.369 \times 10^{-3}$	$3.153 \times 10^{-3}$	-6.4
3	33.06	$8.983 \times 10^{-4}$	$8.371 \times 10^{-4}$	-6.8
<i>Mg / Ca</i>				
1	77.76	$5.888 \times 10^{-3}$	$6.036 \times 10^{-3}$	2.5
2	54.32	$2.158 \times 10^{-3}$	$2.226 \times 10^{-3}$	3.2
3	79.54	$6.941 \times 10^{-3}$	$6.497 \times 10^{-3}$	-6.4
<i>Ca</i>				
1	63.62	$3.761 \times 10^{-3}$	$3.340 \times 10^{-3}$	-11.2
<i>Calibration equations:</i>				
Zn-MTB:		$\Delta t = 22.871 \ln[\text{Zn}] + 282.76$		
HCl-NaOH:		$\Delta t = 11.256 \ln[\text{NaOH}] + 94.883$		
Mg/Ca-EDTA:		$\Delta t = 0.892 \ln[\text{Mg}]^2 + 33.508 \ln[\text{Mg}] + 225.69$		



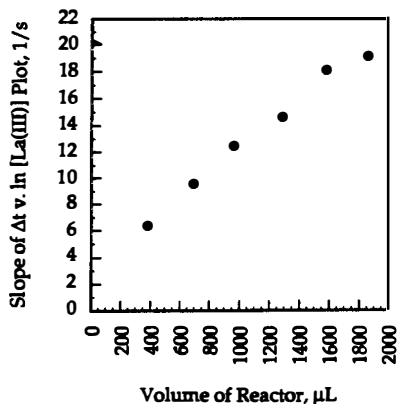


Fig. 3. Change in the slope of  $\Delta t$  vs.  $\ln[\text{La(III)}]$  plots as a function of volume of the alternating helical reactor. The linear relationship of  $V/Q$  and  $V$  confirms the applicability of Eqn. 1 to AHRs.

placed in the reactor, or by decreasing the flow rate. An approximate value for the slope can be determined based solely on the number of segments of the alternating helical reactor; a plot of slope versus the number of reactor segments would be similar to Fig. 3.

#### Flow-injection titrations using alternating helical reactors

Results of FI titrations are listed in Table 4. Calibration plots were constructed from standard solutions of  $\text{Zn(II)}$ ,  $\text{NaOH}$  and  $\text{Mg(II)}$ . Regres-

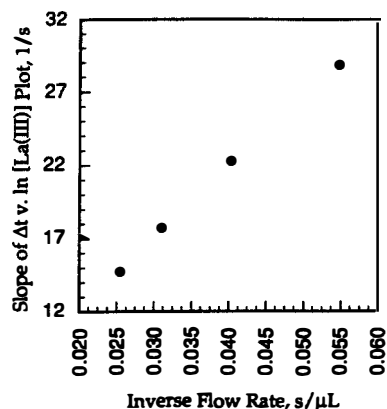


Fig. 4. Change in the slope of  $\Delta t$  vs.  $\ln[\text{La(III)}]$  plots as a function of the inverse of the flow rate. The linear relationship of  $V/Q$  and  $1/Q$  confirms the applicability of Eqn. 1 to AHRs.

sion equations from the calibration data are noted at the bottom of the table. The results show that the doublet peak width FI method can be used quantitatively for simple determinations. Percent differences in the determined concentrations of the unknowns in Table 4 are both positive and negative. The 95% confidence interval of the mean percent difference includes zero:  $-2.2 \pm 2.4\%$ . Thus, there is no experimental bias in the results. Errors in determined concentrations are a result of random error and can be improved by decreasing the uncertainty in the measurement of  $\Delta t$  (see discussion of uncertainty below).

The chemical systems illustrated in this work are examples of the determinations using FI titrations. As noted by Ramsing et al. [6], many titrimetric methods can be applied to FI titrations. For example, EDTA can be used as a titrant for many metals in the same manner as that described for  $\text{Mg}$  and  $\text{Ca}$ . Organic reagents such as pyrocatechol violet, xylenol orange, arsenazo III and alizarin complexone may be used in simple reactions like that described for MTB. Chemical interferences and competing side reactions can be overcome by the same procedures used in standard titrimetric methods [23].

For the  $\text{Mg}/\text{Ca}$ -EDTA system, the regression equation based on  $\text{Mg}$  standard solutions was applicable for solutions containing both  $\text{Ca}$  and  $\text{Mg}$ . The unknown solution that contained no  $\text{Mg}$  was the greatest in error. This is in keeping with the general philosophy of the water-hardness titrimetric method, that  $\text{Mg}$  is required for a sharp endpoint [23]. Other experimental similarities to the standard titrimetric method should be noted: As EDTA penetrates the injected solution slug (free  $\text{Mg}$ , free  $\text{Ca}$  and  $\text{Mg}$ -calmagite), it first reacts with the free  $\text{Ca}$ , then with the free  $\text{Mg}$  and finally with the complexonate. An alternative way to determine  $\text{Mg}$  in this FI system would be to use a buffered carrier stream of the calmagite indicator (as with the  $\text{Zn}$ -MTB method), but it would not be possible to determine the total water-hardness with such a reaction.

The indirect manner in which the  $\text{Mg}/\text{Ca}$ -EDTA reaction is monitored might be the cause of the slight nonlinearity in the regression plot. The concentration-time profile of the indicator is

not the same as that of the analyte. During the reaction EDTA displaces calmagite from the metal and the blue-colored free ligand is monitored spectrophotometrically. At the pair of points of highest EDTA penetration into the Mg/Ca injected slug, the concentration of calmagite reaches a maximum; these points are the peaks for the doublet. As was discussed above, it is assumed that the product absorbance–time profile follows that of the sample. For this reaction, it is further assumed that the indicator concentration–time profile is following the product profile. Diffusion effects and the time for the ligand exchange reaction to occur are sources of error which may lead to the nonlinearity of the plot. An advantage of this method is that broad second peaks, which are associated with the injection of high concentration sample solutions, are avoided. This is a result of adding fewer moles of indicator to the analyte solution than there are moles of metal. By adjusting the concentration of the indicator and the carrier, the working range of the method can be established at higher concentrations than those employed in this work.

#### Discussion of uncertainty

Discussions of the uncertainty in an instrumental procedure are often formulated in terms of a discussion of the precision of the instrument response (occasionally in terms of the uncertainty in response as a function of concentration) and usually ignore the contribution to the uncertainty caused by the need to interpolate from a calibration plot.

For methods based on a logarithmic function of concentration, an increase in the uncertainty in concentration may be expected. For Eqn. 1, the standard deviation of an  $\Delta t$  value,  $s_{\Delta t}$  is related to the standard deviation in concentration,  $s_{C_s}$ , by the following equation [19,24]:

$$s_{\Delta t} = (d[V/Q \ln C_s]/dC_s)s_{C_s} \quad (2)$$

The relative standard deviation in concentration is expressed as

$$s_{C_s}/C_s = (Q/V)s_{\Delta t} \quad (3)$$

$Q/V$  is the inverse of the slope for the plot of Eqn. 1. For the coiled tubing reactor, the 60 cm

single-bead string reactor and the 3-segment alternating helical reactor, standard deviations in  $\Delta t$  are no greater than 0.3 s and thus relative standard deviations in concentration would be calculated as 5.7%, 6.6% and 4.8%. The high error in concentration is expected because the slopes of the  $\Delta t$ – $\ln C_s$  plots for these reactors are quite small. For the 18-segment AHR, the relative standard deviation would be 1.6%. However, this error treatment underestimates the overall uncertainty of the method as no account has been taken of the uncertainty in the slope of the calibration.

The standard deviation ( $s_{x_o}$ ) of a determined concentration can be approximated using the following general equation [19,21]:

$$s_{x_o} = s_{y/x}/b \left\{ 1/m + 1/n + (y_o - \bar{y})^2 / b^2 \sum (x_i - \bar{x})^2 \right\}^{1/2} \quad (4)$$

The concentration of interest ( $x_o$ ) is calculated from  $y_o$ , which is a mean value based upon  $m$  replicates,  $s_{y/x}$  is the standard error of the estimate,  $b$  is the slope of the calibration plot,  $x_i$  values are the individual  $x$  values obtained from a regression based on  $n$  data points, and  $\bar{x}$  and  $\bar{y}$  are the mean data points used in the regression. For this work, all  $x$  in Eqn. 4 represent  $\ln C_s$  values and all  $y$  represent  $\Delta t$  values. A confidence interval (CI) can be calculated for  $s_{x_o}$  as  $x_o \pm ts_{x_o}$  ( $t$  values of 95%,  $n - 2$  are used). Typical values for the NaOH and Zn determinations (Table 4) will be used as examples.

For NaOH Unknown 4,  $s_{x_o}$  is 0.043. The CI of  $\ln[\text{OH}^-]$  is  $-5.369 \pm 0.093$ , which corresponds to an  $\text{OH}^-$  concentration CI of  $4.245 \times 10^{-3} \text{ M} < [\text{OH}^-] < 5.113 \times 10^{-3} \text{ M}$ . For Zn Unknown 4,  $s_{x_o}$  is 0.027. A  $\ln[\text{Zn(II)}]$  CI of  $-7.067 \pm 0.089$  corresponds to a Zn(II) concentration CI of  $7.805 \times 10^{-4} \text{ M} < [\text{Zn(II)}] < 9.318 \times 10^{-4} \text{ M}$ . The concentration CI is not symmetric around the determined concentration as a result of the logarithmic function. The CI of NaOH Unknown 4 encompasses percent differences of  $-8.9\%$  and  $+9.6\%$ ; the CI of Zn Unknown 4 encompasses percent differences of  $-8.5\%$  and  $+9.3\%$ .

On the basis of the treatment of uncertainty discussed above, the FI titration results shown in

Table 4 are as good as can be expected without (a) improvements in the precision in the measurement of time, (b) an increase in the slope of the  $\Delta t - \ln C_s$  plot and (c) improvement in the fit of the points to a straight line function, if an unweighted least squares procedure is to be used to establish the slope of the calibration function. In considering the mixing devices used in this paper, it is the magnitude of the slope, rather than the error in the  $\Delta t - \ln C_s$  plots that is most important in reducing the error in these determinations. Several mixing devices had low  $s_{y/x}$  values, but had a flat calibration plot as compared to that of the AHRs. This conclusion bolsters the argument made above for choosing the alternating helical reactor as the best static mixer. Use of slower flow rates and larger volume AHRs will result in smaller relative standard deviations in determined concentrations. Limiting the calibration range to reduce errors in locating the absorbance maxima for concentrated solutions should further reduce errors in determinations.

### Conclusions

Alternating helical reactors are the mixing devices that are suitable alternatives to the well-stirred tank for FI systems designed to produce doublet peaks. The straight-line fit of the data, the relatively steep slopes of the  $\Delta t - \ln C_s$  plots and the ease of construction of the AHRs make these reactors a practical choice for FI methods based on the time interval between doublet peaks. The slope of the calibration plots may be varied by adjustment of the reactor volume and flow rate.

The time interval between doublet peaks are accurately and easily obtained from the output of an integrator and can be used to determine metal ions in simple matrices. Three simple chemical systems illustrate the type of reactions that may be used for these FI time-based methods (FI titrations). The working range of the calibration plots are not as great as those reported previously, but are between two to three orders of magnitude. Errors in concentration that results from a calibration plot of doublet peak time intervals are reasonable. The slope of the calibra-

tion plot is important for obtaining low relative standard deviations for determined concentrations. The best experimental parameters for determinations based on doublet peak widths are large volume AHRs and relatively slow flow rates.

Financial support from Pfizer Inc. (Groton, CT) is gratefully acknowledged.

### REFERENCES

- 1 J. Ruzicka and E.H. Hansen, *Flow Injection Analysis*, Wiley, New York, 2nd edn., 1988.
- 2 M. Valcarcel and M.D. Luque de Castro, *Flow-Injection Analysis*, Ellis Horwood, Chichester, 1987.
- 3 J. Ruzicka, E.H. Hansen and H. Mosbaek, *Anal. Chim. Acta*, 92 (1977) 235.
- 4 J.F. Tyson, *Analyst*, 112 (1987) 523.
- 5 J.F. Tyson, *Anal. Chim. Acta*, 179 (1986) 131.
- 6 A.U. Ramsing, J. Ruzicka and E.H. Hansen, *Anal. Chim. Acta*, 129 (1981) 1.
- 7 J. Bassett, R.C. Denney, G.H. Jeffrey and J. Mendham, *Vogel's Textbook of Quantitative Inorganic Analysis*, Longman, New York, 2nd edn., 1978.
- 8 H.L. Pardue and B. Fields, *Anal. Chim. Acta*, 124 (1981) 39.
- 9 H.L. Pardue and B. Fields, *Anal. Chim. Acta*, 124 (1981) 65.
- 10 H.L. Pardue and P. Jager, *Anal. Chim. Acta*, 179 (1986) 343.
- 11 P. Jager and H.L. Pardue, *Anal. Chim. Acta*, 187 (1986) 343.
- 12 H.L. Pardue, *Anal. Chim. Acta*, 220 (1989) 23.
- 13 J.M. Jordan and H.L. Pardue, *Anal. Chim. Acta*, 270 (1992) 204.
- 14 J.M. Jordan, S.H. Hoke and H.L. Pardue, *Anal. Chim. Acta*, 272 (1993) 115.
- 15 J.F. Tyson, *Analyst*, 112 (1987) 527.
- 16 M.K. Carroll and J.F. Tyson, *J. Chem. Educ.*, 70 (1993) A210.
- 17 M.K. Carroll, A. Murfin and J.F. Tyson, *Anal. Chim. Acta*, submitted for publication.
- 18 M.K. Carroll and J.F. Tyson, *Appl. Spectrosc.*, in press.
- 19 A. Wynne, personal communication.
- 20 J.C. Miller and J.N. Miller, *Statistics for Analytical Chemistry*, Ellis Horwood, Chichester, 3rd edn., 1993.
- 21 L.S. Serdyuk and V.S. Smirnaya, *Zh. Anal. Khim.*, 20 (1965) 161.
- 22 B. Budesinsky and E. Antonescu, *Collect. Czech. Chem. Commun.*, 28 (1963) 3264.
- 23 A. Ringbom, *Complexation in Analytical Chemistry*, Robert E. Krieger Publishing Co., New York, 1979.